Blockage of IL-17 Ameliorates Aβ-Induced Neurotoxicity and Cognitive Decline

Yulan Liu
Wuhan University Renmin Hospital
Yang Meng
Renmin Hospital of Wuhan University: Wuhan University Renmin Hospital
Chenliang Zhou
Renmin Hospital of Wuhan University: Wuhan University Renmin Hospital
Wenfang Xia
Renmin Hospital of Wuhan University: Wuhan University Renmin Hospital
Lu Wang
Renmin Hospital of Wuhan University: Wuhan University Renmin Hospital
Juanjuan Yan
Renmin Hospital of Wuhan University: Wuhan University Renmin Hospital
Li Cheng
Renmin Hospital of Wuhan University: Wuhan University Renmin Hospital
Weiguo Dong (dongweiguo155@sina.com)
Renmin Hospital of Wuhan University: Wuhan University Renmin Hospital
Cuiping Guo
Renmin Hospital of Wuhan University: Wuhan University Renmin Hospital

Research

Keywords: IL-17, Y-320, amyloid-β, neural toxicity, cognitive decline

Posted Date: July 30th, 2021

DOI: https://doi.org/10.21203/rs.3.rs-742937/v1

Abstract

Background

Neuroinflammation plays a critical role in the pathophysiology of Alzheimer's disease (AD), particularly in amyloid-β (Aβ) production. But the impact of the cytokine, interleukin-17A (IL-17) on the course of AD has not been well defined. The goal was to determine the effect of IL-17 on neural damage and whether IL-17 inhibitor (Y-320) could ameliorate Aβ-induced neurotoxicity and cognitive decline.

Methods

The expression level of IL-17 was analyzed in APP/PS1 mice. Then IL-17 was injected into the lateral ventricle of C57BL WT mice and roles on synaptic dysfunction and cognitive impairments were examined. $A\beta_{42}$ was injected into the lateral ventricle of to mimic $A\beta_{42}$ model mice. The effects of IL-17 inhibitor by oral gavage on $A\beta_{42}$-induced neurotoxicity and cognitive decline were examined.

Results

We found that IL-17 was increased in the hippocampus of APP/PS1 transgenic mouse, which has a fundamental role in mediating brain damage in neuroinflammatory processes. Furthermore, we reported that IL-17 was administrated in primary hippocampal neurons, leading to neural damage and synaptic dysfunction. At the same time, IL-17 caused synaptic dysfunction and cognitive impairments accompanying with increased of Aβ levels in mice. In addition, we found that Y-320 could rescue $A\beta_{42}$–induced neural damage in primary hippocampal neurons, and ameliorate neuronal damage and cognitive impairments in $A\beta_{42}$ model mice. Interestingly, we observed that IL-17 upregulated the production of soluble amyloid precursor protein β (sAPPβ) and phosphorylation of APP at T668 (pT668), moreover, Y-320 inhibited the Aβ production by down-regulation the sAPPβ and pT668.

Conclusions

Blockage of IL-17 might ameliorate Aβ-induced neurotoxicity and cognitive decline. These results strongly demonstrate a potential therapeutic role for IL-17 inhibitor in AD.

Background

Alzheimer's disease (AD) is the most common type of dementia and a rising threat for public health [1]. Aggregation and accumulation of amyloid-beta (Aβ) peptide, a hallmark of AD neuropathology, plays a central causal role in the disease progression and is regulated and directly affected by chronic neuroinflammation. [2–4]. Aβ is produced by the cleavage of amyloid precursor protein (APP) via β-site APP cleaving enzyme 1 (BACE1) and γ-secretase, released and deposited into extracellular senile plaques [5]. The majority of secreted Aβ peptides are 40 amino acids ($A\beta_{40}$), and 42 amino acids ($A\beta_{42}$). Aβ assemblies induce synaptic damage, excitotoxicity, and neuronal death and cognitive impairments [6, 7].

APP/PS1 transgenic mice expressing Swedish APP mutation and presenilin-1 mutation mimic pathological features of human disease including neural dysfunction, Aβ deposition and neuroinflammation [8]. Each disease component affects one another. Neuroinflammation is not a passive system activated by Aβ deposition, but instead contributes awfully to pathogenesis of AD [9, 10]. As mediators and modulators of neuroinflammation, cytokines contribute to nearly every aspect of neuroinflammation, including proinflammatory and anti-inflammatory processes, and response of microglia to Aβ deposits. Some studies proved that cytokines such as tumor necrosis factor α (TNF-α) and interleukin-10 (IL-10) impaired neuronal function [11–13]. Conversely, IL-1β, IL-12/IL-23 reduced amyloid plaque pathology, and ameliorate AD-like pathology [14–16].

IL-17 is a pro-inflammatory cytokine produced by various types of cells including CD4 T cells which are categorized as a new subset called Th17 cells. It is participated in the development of autoimmunity, inflammation and tumor immunity and plays a role in the host defense against bacterial and fungal infections [17, 18]. It is interesting to note that plasma IL-17 level has been identified as one of the plasma biomarkers for AD diagnosis and neocortical Aβ load [19, 20]. However, some studies also suggested that IL-17 may decrease Aβ levels in the brain and promoted sociability in mice model of neurodevelopmental disorders [21, 22]. So the effect and specific mechanism of IL-17 in neurodegenerative disease is still unclear.

In this study, we investigate the effect of IL-17 via lateral ventricle delivery on neural toxicity, cognitive impairment and $A\beta_{42}$ levels. Furthermore, we explore the potential ability of IL-17 inhibitor (Y-320) to reduce the neuropathological alterations that are present in $A\beta_{42}$ induced AD-like pathology in mice model.

Materials And Methods

Animals and reagents

Wild type (WT) C57BL mice (2 months old, male) and APP/PS1 (expressing familial AD mutants of APP and presenilin-1, 6 months old, male) mice were purchased from Beijing Huafukang Biological Technology Co. Ltd. Mice were housed in Experimental Animal Central of Renmin Hospital of Wuhan University under standard laboratory condition: 12-h light and 12-h dark with water and ad libitum food. Mice were randomly divided into groups and treated as explained in different parts of the study. IL-17 group mice were administered by lateral ventricle injection with IL-17 (100 μg/mL; 5 μL; R&D Systems, Minneapolis, MN) for 7 days. All animal experiments were approved by the Institutional Animal Care and Use Committee at Renmin Hospital of Wuhan University.

Y-320 (Selleck, Houston, TX) [23], the inhibitor of IL-17, was administrated to each animal at a dose of 3 mg/kg per day by oral gavage for 7 consecutive days. Y-320 was dissolved in dymethyl sulfoxide (DMSO), according to the manufacture's instruction.

Enzyme-linked immunoSorbent assays (Elisa)

Anti-mouse IL-17, IL-1β, IL-6, TNF-α Elisa kits from Elabscience Biotechnology (Wuhan, China) were used to assay hippocampus cytokine levels, according to the manufacturer's instructions. ELASA kits were also used to measure $A\beta_{40}$, $A\beta_{42}$ (Amyloid beta 40 and 42 Mouse ELISA Kits, ThermoFisher) in brain samples.

Stereotactic surgery

The intracerebroventricular surgery was performed as follows: anterior-posterior: -0.3mm; mediolateral: -1 mm; dorsoventral: -2.3 mm (from bregma and dura, flat skull). After injection, the needle was kept in place for 10 minutes to avoid flow back of solution.

$A\beta_{42}$ (Qiangyao Biotechnology) was oligomerized according to the procedure described previously [24, 25]. In brief, the $A\beta_{42}$ was dissolved in DMSO and diluted in physiological saline to a final concentration of 2.0 μg/μL. Then, the solution was incubated at 37°C in dark for one week before use. The mice were anesthetized with isoflurane and placed in a stereotaxic apparatus. And, the mice were injected through brain lateral ventricle, with the solution with $A\beta_{42}$ (5 μL), and the control group was injected with same volume of sterile normal saline containing DMSO (1%).

Western blotting

The hippocampi were homogenized in a buffer (pH 7.4) containing 50 mmol/L Tris-HCl, 150 mmol/L NaCl, 10 mmol/L NaF, 1 mmol/L Na_3VO_4, 5 mmol/L EDTA, 2 mM benzamidine, and 1 mM PMSF. The supernatants were collected after centrifugation of the tissue homogenates or cell lysate at 12000 rpm/min. Protein concentrations were determined with the bicinchoninic acid protein kit (Pierce, Rockford, IL, USA). Equal amounts of protein were loaded onto 10% gel (Invitrogen, Bis-Tris), separated by electrophoresis, and then transferred to a PVDF membrane. The images were visualized with an Odyssey infrared imaging system (LI-COR Biosciences, USA). For western blotting, the primary antibodies used were IL-17 (1:1000; Cell Signaling Technology, USA), synaptophysin (SYN, 1:1000, Abcam, USA), postsynaptic density protein 95 (PSD-95, 1:1000, Abcam, USA), soluble amyloid precursor protein β (sAPPβ, 1:1000; Abcam, USA), phosphorylation of APP at T668 (pT668, 1:1000; Abcam, USA), and actin (1:1000; Abcam, USA). Secondary antibodies were horseradish peroxidase conjugated to mouse anti-rabbit/mouse immunoglobulin G (1:10,000, Sigma, MO).

Primary neuron culture

Primary hippocampal neurons were dissected from the brains of E18 Sprague-Dawley rat embryos according to previously described procedures with minor modifications [26]. Neurons were cultured in 6-well plates at a density of 5×10^5 per well coated with 100 ug/mL poly-D-lysine and supplemented with 2% (v/v) B-27 and 1× GlutaMAX. The neurons were cultured for nine days were used in experiments. In the experiment, the cells were divided into several groups: control group, IL-17 group (IL-17, 10 μg/mL), $A\beta_{42}$ group ($A\beta_{42}$, 2.5 μM) and $A\beta_{42}$ + IL-inhibitor ($A\beta_{42}$, 2.5 μM; Y-320, 100 nM). At the end of treatments, cells were collected and lysed in RIPA buffer for further biological detection or fixed with 4% paraformaldehyde (PF) for immunofluorescence imaging. All cell culture reagents were purchased from Thermo Fisher Scientific.

Immunofluorescence staining

Hippocampal neuronal cells were rinsed with PBS and fixed in 4% PF for 20 min and permeabilized with 0.1% Triton X-100 in PBS for 30 min. After blockade with 5% normal goat serum for 30 min, cells were incubated with primary antibodies conjugated to alexa-fluo®488 or 594 against: microtubule-associated protein-2, (MAP2, 1:250, Abcam), PSD-95 (1:250, Cell signaling Technology) at 4°C overnight. The second antibody was then incubated at room temperature for 1 hour, and then rinsed in PBS for three times. The nucleus was stained by DAPI (Sigma-Aldrich) for 5 min. Fluorescence images were obtained using a BX51 Olympus fluorescence microscope or a FV1200 Olympus laser-scanning confocal microscope. Sholl analysis was applied to measure dendritic complexity as recorded previously [27]. The length of dendritic arborization was analyzed and measured using semi-automatized protocol via Imaris software (Bitplane, Inc.)

Behavior test

Open field

The open field is used to assess tension, anxiety, and exploration activities of experimental animals. In brief, experimental mice were placed in a typical open field, and movements inside the field were tracked over the period of 5 min. The total distance covered and central zone crossing were tracked and measured. The chamber was cleaned with 70% ethanol after each trial.

Novel objective recognition test (NORT)

The mice were taken to the new object recognition room 24 h before the test, and then we put the mouse into a 100 cm × 100 cm ×100 cm plastic container for 5 min without objects prior to the test. The day after the mice re-entered the container the same starting point and were allowed for 5 min to familiarize themselves with A and B objects. After each period, the arena and objects were cleaned with 75% ethanol. Two hours after the familiarization period, the B object was replaced by the C object, and the mice were granted 5 min to explore the both objects. After 24 h, the C object was replaced with D object, and the mice were also given 5 min to explore. The exploring time on each object was recorded.

Contextual fear conditioning

The scene memory function of the mice was further detected by fear conditioning test. Mice were placed into a square chamber (40cm × 40 cm × 50 cm) with white board walls, a transparent front door, and grid floor. On the day of training, the mice were allowed to explore in an enclosed training chamber for 180 s. The mice were then exposed to a pure tone for 30 s, followed by a 2-s foot shock (0.8 mA). At 60 s after delivery of the second shock, the mice were returned to their home cages. 24 hours later, mice were sent into the same chamber for 3 min without foot shock for fear memory test. The time of freezing was measured using the Contextual NIR Video Fear Conditioning System (Med Associates).

Morris water maze test (MWM)

Spatial learning and memory were detected by MWM as described in a previous study. The MWM consists of a propylene round pool (120 cm in diameter and 50 cm deep) virtually divided in four equal quadrants. A platform (10×10×15 cm) was placed into the pool, 1.5 cm below the water surface and 10 cm from the wall. The water was made opaque by adding white titanium dioxide. The following protocol was applied. The mice were trained to find a hidden platform for 5 consecutive days. In each trial, the mouse started from one of four quadrants facing the wall of the pool and ended when the mouse climbed on the platform with maximum trial duration of 60 s. Latency time to find the hidden platform was recorded during each trial of each learning session. If the mouse found the platform within the maximum trial time allowed, it was left on the platform for 20 s. If the mice did not find the platform within the time limit, it was gently placed on the platform for a 20 s period. The test was carried on the next day after training. The platform was removed and the latency of first crossing of platform, the number of crossing, and the time in target quadrant were recorded for 60 s.

Long-term potentiation (LTP)

In brief, after the mice were sacrificed, whole brains were immediately resected and soaked in ice-cold aCSF saturated with 95% O_2 and 5% CO_2. Following sectioning at 300-μm thickness, the slices were incubated in oxygenated aCSF at 32°C to recover for 40 min and at 20–25°C to recover for 1 h. Then slices were transferred to a recording chamber and submerged in aCSF perfusion. Slices were laid down in a chamber with an 8 × 8 microelectrode array (Parker Technology, Beijing, China) in the bottom planar (each 50 × 50 mm in size, with an interelectrode distance of 150 μm) and kept submerged in aCSF. Signals were acquired using the MED64 System (Alpha MED Sciences, Panasonic). The field excitatory postsynaptic potential (fEPSP) in CA1 neurons were recorded by stimulating CA3 neurons. LTP was induced by applying three trains of high-frequency stimulation (100 Hz for 1 s, delivered 30 s apart). The LTP magnitude was quantified as the percentage change in the fEPSP slope (10%-90%) taken during the 60-min interval after LTP induction.

Transmission electron microscopy (TEM)

After perfusion with fixatives as described above hippocampi were dissected out and slices approximately 150 μm thick. The slices were fixed further by immersion in 0.1 M Na-cacodylate buffer containing 2.5% glutaradehyde for 1 h at room temperature. Postfix with 1% OsO4 in 0.1 M PBS for 2 h at room temperature. Then dehydrate and infiltrate. Sections were photographed under light microscope and then serially cut into semithin (2 μm thick) sections. The semithin sections were stained with 1% toluidine blue in 1% sodium borate, examined under the light microscope to locate CA1 region. Selected semithin sections were further cut into serial ultrathin sections using a Leica ultramicrotome. The ultrathin sections were examined under a HITACHI HT7800 TEM by an electron microscopy specialist from the Department of Ultrastuctural Pathology Center, Renmin Hospital of Wuhan University. Synaptic densities were expressed as number of synapses (identified via PSDs), per 100 μm^2 of tissue.

Golgi staining

FD Rapid Golgi Staining Kit PK 401(FD NEUROTECHNOLOGIES, INC, Columbia MO, USA) was used to measure the morphology of neuronal dendrites and dendrites' spines. The mice were anesthetized by isoflurane and transcardially perfused with proximately 400 ml of normal saline containing 0.5% sodium nitrite, followed with 400 ml 4% formaldehyde solution and then 500 ml Golgi dye solution (5% chloral hydrate, 5% potassium dichromate, and 4% formaldehyde) over 2 h. And then, brains were dissected into 5 mm × 5 mm sections and incubated in the staining solution for 3 days and in 1% silver nitrate solution for another 3 days in the dark. Finally, the brains were sliced using a vibrate microtome (Leica, Wetzlar, Germany) at a thickness of 100 μm. Images were observed under the microscope (BX51 Olympus fluorescence microscope, Japan).

Statistical Analysis

All experiments were repeated at least three times. Data were expressed as mean ± SEM and analyzed using GraphPad Prism. The significance of differences was assessed by the Student's test or one way ANOVA followed by the Bonferroni post hoc test as indicated. $P < 0.05$ was considered statistically significant in all experiments.

Results

IL-17 is up-regulated in APP/PS1 transgenic mice and induces neural toxicity.

Previous studies suggested critical roles for inflammatory cytokines in the pathogenesis of AD [11, 13, 28]. To analyze the expression of IL-1β, IL-6, TNF-α and IL-17 in amyloidosis-prone APP/PS1 mice, we performed ELASA test of 6-month-old APP/PS1 mice hippocampus. The expressions of IL-1β, IL-6, TNF-α (sFig. 1A-C) and IL-17 (Fig. 1A) were increased in hippocampus of APP/PS1 mice when compared to controls. Furthermore, analysis of western blotting from APP/PS1 mice hippocampus also showed significantly increased level of IL-17 (Fig. 1B, C). However, specific mechanism of IL-17 in neurodegenerative disease is still controversial. We then try to investigate the mechanism of IL-17 on AD-like pathology by observing the effect on neural in primary hippocampal neurons. The hippocampal primary neurons were divided into control group and IL-17 group (IL-17, 10 μg/mL). When compared with the control, IL-17 treatment resulted in an obvious decreased dendritic arborization complexity at all points farther than 60 um from the cell body (Fig. 1D-F). These data indicate that IL-17 may play a pathophysiological role in neural toxicity.

IL-17 results in cognitive and memory impairments and synaptic dysfunction accompanying with Aβ overproduction.

Thirty healthy wild type C57BL mice were adaptively domesticated for 7 days in animal laboratory. Then the mice were randomly divided into 2 groups (control and IL-17 group) of 15 each. The IL-17 group mice were injected with IL-17 for 1 week by intracerebroventricular surgery, and saline served as control for 1 week. We first carried open-field test after injection and the result showed that there was no significant difference in the total distance covered between the two groups (Fig. 2A), but the time of center duration

was significantly reduced in IL-17 group compared with the control (Fig. 2B), implicating that IL-17 might reduce the ability of exploration. To further observe the exploration and short-term memory capacity in the mice, we employed novelty recognition experiments and found that the curiosity in IL-17 group was significant reduced, as the time spent for exploration of new object in 2h and 24h were significantly decreased (Fig. 2C, D). To examine the scene memory of the mice, we carried out the contextual fear conditioning test and found out that the scene memory was significantly impaired in the test group (Fig. 2E, F). Finally, we tested memory and learning abilities using MWM, and observed that there was no significant difference in the speed, but significantly increased latency to find the hidden platform between the two groups (Fig. 2G, H). On day 6, the spatial memory was checked by removing the platform. A remarkable decrease in the time spent in the target quadrant (Fig. 2I), as well as a decrease in the number of target platform crossing (Fig. 2J), was observed in the IL-17 group mice.

It is clear that IL-17 results in a series of cognitive and memory impairments in mice. Among these behavioral alterations, learning and memory impairments are commonly shared with other neurological disorders including neurodegenerative disease [29]. And the above result showed that IL-17 level was up-regulated in APP/PS1 mice. The hippocampus is an integral part of the temporal limbic system and plays a critical role in memory and spatial location which is the reflection of synaptic plasticity [30, 31]. We wondered whether IL-17 might increase Aβ levels and then lead to synaptic dysfunction. Interestingly, the $A\beta_{40}$ and $A\beta_{42}$ in hippocampus were significantly higher in IL-17 group mice than in the control ones (Fig. 3A, B). We further investigated the levels of sAPPβ and pT668. The results showed that the levels of sAPPβ and pT668 in IL-17 group were increased compared with control group (sFig. 2A -C). Moreover, IL-17 dramatically caused the LTP impairment of mice (Fig. 3C, D), suggesting impaired synaptic function in IL-17 mice. To investigate the underlying mechanism, we further observed the ultrastructure of synapse in hippocampus with TEM, and results showed that the number of synapses per 100 um^2 CA1 areas decreased significantly after IL-17 injection (Fig. 3E, F). We further examined the spine density of hippocampus neurons (Fig. 3G). The Golgi staining showed a significant decrease in the dendritic spine density of the IL-17 mice (Fig. 3H). In addition, we further performed western blotting and the result from the IL-17 groups showed a significant reduction in the synaptic protein levels of SYN and PSD95 (Fig. 3I, J). These results together imply that IL-17-induced cognitive impairments are associated with synaptic dysfunction accompanying with Aβ overproduction.

IL-17 inhibitor (Y-320) ameliorates $A\beta_{42}$-induced neural toxicity in primary hippocampal neurons.

We have shown that IL-17 could induce cognitive impairment and synaptic dysfunction, an effect that may be mediated via increasing Aβ level. Aβ oligomers now widely regarded as instigating neuron damage leading to Alzheimer's dementia [32, 33]. To further confirm this hypothesis, we performed an inhibitor of IL-17 (Y-320) to investigate whether it could ameliorate $A\beta_{42}$-induced neural toxicity in primary hippocampal neurons at first. In the experiment, the hippocampal primary neurons were divided into three groups: control group, $A\beta_{42}$ group ($A\beta_{42}$, 2.5 μM), $A\beta_{42}$ + IL-17 inhibitor group ($A\beta_{42,}$ 2.5 μM; Y-320, 100 nM). Y-320 resulted in a robust increase in the dendritic complexity at all points farther than 60μm from

the cell body when compared with $A\beta_{42}$ treated neurons (Fig. 4A -C). These data indicate that IL-17 inhibitor may ameliorate $A\beta_{42}$-induced neural toxicity.

IL-17 inhibitor alleviates Aβ $_{42}$ -induced cognitive and memory Deficits in mice.

Studies using the $A\beta_{42}$ human peptide showed impaired cognitive function early after a single intracerebroventricular injection [24, 34]. Based on the primary neuron results, we explored the effect of IL-17 inhibitor in $A\beta_{42}$ model in *vivo*. We used 45 healthy C57BL mice randomly divided into 3 groups. Control group mice injected with saline (5 μL) in brain unilateral ventricle. $A\beta_{42}$ mice model was established after injecting in brain unilateral ventricle with the solution $A\beta_{42}$ (2.0 μg/μL, 5 μL), while the IL-17 inhibitor group were injected with $A\beta_{42}$ (2.0 μg/μL, 5 μL), followed with oral gavage treatment of Y-320 (3 mg/kg, 7 days). Following the treatment, we again performed a couple of behavioral tests. In the open-field test, total distance showed no significant difference among three groups (Fig. 5A), indicating that the locomotion activity was not influenced by $A\beta_{42}$ and Y-320 treatment. But the time of center duration was significantly increased in $A\beta_{42}$ + IL-17 inhibitor group compared with the $A\beta_{42}$ group. Next, the NORT showed that IL-17 inhibitor could significantly lengthen the time of new object spent by $A\beta_{42}$ model mice in 2h and 24h (Fig. 5C, D). And then, the contextual fear conditioning test were performed and found out that the scene memory of mice was alleviated in $A\beta_{42}$ + IL-17 inhibitor group compared with $A\beta_{42}$ model group (Fig. 5E, F). Last, in MWM, the escape latency was significantly increased in the $A\beta_{42}$ group compared with the control group on day 2, 3, 4 and 5, while supplementation with Y-320 attenuated $A\beta_{42}$-induced learning deficits (Fig. 5H). In the probe trial on day 6, time was remarkably increased in the target quadrant (Fig. 5I) and the crossing number of target platform was increased (Fig. 5J) in $A\beta_{42}$ + IL-17 inhibitor group. These behavioral tests results suggest that IL-17 inhibitor alleviates $A\beta_{42}$-induced learning and memory deficits in mice.

IL-17 inhibitor rescues Aβ $_{42}$ -induced spine loss and synaptic dysfunction by reducing Aβ production.

We have previously found that IL-17 leads to synaptic dysfunction accompanying with up-regulation levels of $A\beta_{40}$ and $A\beta_{42}$ in hippocampus (Fig. 3). To further explore the relationship between IL-17 and Aβ, we supplied Y-320 in $A\beta_{42}$ model mice. Western blotting and Elisa test showed the level of IL-17 was increased in $A\beta_{42}$ model mice compared with control group, and reversed by IL-17 inhibitor treatment (Fig. 6A-C). We also tested $A\beta_{40}$ and $A\beta_{42}$ by Elisa and the results showed in hippocampus the levels were significant increased in $A\beta_{42}$ model group and attenuated after supplementation with Y-320 (Fig. 6D, F), again suggesting that IL-17 inhibitor could be a protective element against the pathogenesis of Aβ toxicity. We further investigated the possible mechanism underlying the effect of IL-17 inhibitor on reducing Aβ production. The results showed that the levels of sAPPβ and pT668 in $A\beta_{42}$ + IL-17 inhibitor group were decreased compared with $A\beta_{42}$ group (sFig. 3A-C). In view of the above data, we wonder whether the IL-17 inhibitor plays a positive role in synaptic dysfunction induced by $A\beta_{42}$. We therefore carried out electrophysiology experiments and found that IL-17 inhibitor enhanced the slope of fEPSP

produced by mice in $A\beta_{42}$ model group (Fig. 7A, 7B). In addition, we observed the number of synapses in hippocampus with TEM, and results showed that the number of synapses per 100 μm^2 CA1 areas increased significantly after IL-17 inhibitor supplement compared with $A\beta_{42}$ model group mice (Fig. 7C, D). And $A\beta_{42}$ injection resulted in significant dendritic spine loss revealed in Golgi staining, and IL-17 inhibitor effectively reversed the spine loss (Fig. 7E, F). Consistent with these findings, the levels of SYN and PSD95 were reduced in $A\beta_{42}$ group and partially recovered after supplementation with Y-320 (Fig. 7G-I). These results indicate that IL-17 inhibitor rescues the $A\beta_{42}$–induced synaptic dysfunction probably by reducing Aβ generation.

Discussion

Neuroinflammation plays a critical role in the pathophysiology of AD. Investigating the role of neuroinflammation is necessary to enhance our understanding of initiation and progression of AD. In this study, we demonstrated that APP/PS1 mice presented an altered hippocampal inflammatory milieu characterized by increased levels of pro-inflammatory mediators IL-17, IL-1β, IL-6, and TNF-α, which may play important roles in the progression of AD neuropathology and cognitive impairments. Among these mediators, we focused on IL-17 owing to its role in mediating brain damage through its potent pro-inflammatory actions [35, 36]. We demonstrated the role of IL-17 in inducing spine loss and synaptic dysfunction in hippocampus and resulting in cognitive deficits in mice companying with up-regulating expression of Aβ. Furthermore, we explored the effect of IL-17 inhibitor (Y-320) in Aβ mice model of AD. Y-320 treatment ameliorated cognitive behaviors, neuromorphological alterations and synaptic dysfunction probably by reducing the production of Aβ in hippocampus in $A\beta_{42}$ model mice.

IL-17 is a pro-inflammatory cytokine produced by various types of cells including CD4 T which are categorized as a new subset called Th17 cells [37]. Th17 cells are the main cellular mediators responsible for immune-mediated damage that polarize to the site of inflammation in presence of noxious or inflammatory stimuli [37, 38]. However, the effect of cytokine IL-17 still remains poorly defined and very little is known on its pathophysiological role in the regions of the CNS usually compromised in diseases. Some studies showed that IL-17 mediated neuroinflammation in AD phenotypes and neutralization of IL-17 rescued neuroinflammation and memory impairment [22]. However, some studies had opposite results that IL-17 overexpression markedly decreased soluble Aβ levels in the hippocampus, drastically reduced cerebral amyloid angiopathy, and significantly improved learning deficits [21]. Consistent with the cognitive alterations found in AD and in the mouse model of AD, in the present study, the behavior tests showed IL-17 treatment mice displayed profound deficits in their learning and memory abilities. Furthermore, IL-17 dramatically caused the LTP impairment, a significant decrease in the number of synapses, and the dendritic spine density, suggesting impaired synaptic function in IL-17 treatment group mice. And then, we performed a couple of behavioral tests such as the open-field test, NORT, the contextual fear conditioning test, and MWM. These behavioral test results implied that IL-17 inhibitor (Y-320) rescued $A\beta_{42}$-induced cognitive deficits in mice. It is now thought that Aβ oligomers purified from AD brains or synthesized inhibit long-term potentiation, cause synaptic dysfunction, damage dendritic spines

and cause neuronal death [39, 40]. In this regard, we showed herein that the inhibition LTP, synaptic dysfunction, dendritic spines loss were significantly ameliorated by administration of Y-320 compared with $A\beta_{42}$ group. Consistent with our results, several studies have demonstrated that blocking IL-17 reduced brain damage associated to neuroinflammatory processes [36, 41]. Positive results have been obtained from clinical trials with antibodies against IL-17 in psoriasis, rheumatoid arthritis and ankylosing spondylitis [42]. Furthermore, the administration of anti-IL-17 antibodies reduces inflammation and improves the neurological prognosis of different CNS pathologies, like post-stroke neurodegeration, encephalic inflammation [43, 44].

IL-17 increased the levels of $A\beta_{40}$ and $A\beta_{42}$. As expected, levels of $A\beta_{42}$ and IL-17 were significantly higher in $A\beta_{42}$ model mice group compared with the control group, while, its levels were significantly reversed by IL-17 inhibitor treatment. APP can be processed via alternative physiological or amyloidogenic pathways depending on whether cleavage occurs via α secretase or β secretase 1 in neurons, which generates sAPPα or sAPPβ products, respectively [45]. Particularly, phosphorylation of APP at T668 (pT668) increases the Aβ product levels by facilitating exposure to and cleavage by BACE1 in AD patients and transgenic models [46, 47]. pT668 is neuron-specific, and highly expressed in amyloid plaques, and induces neurodegeneration [48]. Of interesting, we examined the activity or expression level of sAPPβ and pT668, and the results suggested that compared with the control group, sAPPβ and pT668 were significantly increased in IL-17 treatment mice, and IL-17 inhibitor reversed the levels of sAPPβ and pT668 increased by $A\beta_{42}$. Our results showed that IL-17 inhibitor might reduce pT668, resulting in amyloid generation reduction in hippocampus neurons. The further mechanism will be explored by our research group.

Conclusions

Taken together, blockage of IL-17 might ameliorate Aβ-induced neurotoxicity and cognitive decline. Our findings provide new clues for the mechanism of neuroinflammation reduced-cognitive impairments, and a basis for therapeutic intervention. These results strongly demonstrate a potential therapeutic role for IL-17 inhibitor in AD.

Abbreviations

AD, Alzheimer's disease; Aβ, Amyloid-β; IL-17, Interleukin-17A; APP, Amyloid precursor protein; BACE1, β-site APP cleaving enzyme 1; IL-1β, Interleukin 1β; TNF-α, Tumor necrosis factor α; CTR, Control; WT, wild type; Elisa, Enzyme-linked ImmunoSorbent assays; DMSO, Dymethyl sulfoxide; SYN, Synaptophysin; PSD-95, Postsynaptic density protein 95; sAPPβ, Soluble amyloid precursor protein β; pT668, Phosphorylation of APP at T668; NORT, Novel objective recognition test; MWM, Morris water maze test; LTP, Long-term potentiation; fEPSP, Field excitatory postsynaptic potential; TEM, Transmission electron microscopy.

Declarations

Ethics approval and consent to participate

All animal experiments were approved by the Institutional Animal Care and Use Committee at Renmin Hospital of Wuhan University, and performed in compliance with the National Institutes of Health Guide for the Care and Use of Laboratory Animals.

Consent for Publication

All authors consented to publication of this work.

Availability of data and materials

The datasets used and analyzed during the present study are available from the corresponding authors.

Competing interests

The authors declare that they have no competing interests.

Funding

This work was supported in parts from the National Natural Science Foundation of China (No.8187032070) and the Fundamental Research Funds for the Central Universities (No.2042019kf0081).

Authors' contributions

WD and CG planned, organized, and designed all experiments. YL and YM planned and performed all experiments, including the writing of the manuscript. CZ and WX assisted with the manuscript preparation. JY, LC analyzed the data. All authors read and approved the final manuscript.

Acknowledgements

The authors would like to thank Yingxia Jin and Lina Zhou from Central Laboratory, Renmin Hospital of Wuhan University, for their technical assistance.

Authors' information

[1]Department of Gastroenterology, Renmin Hospital of Wuhan University, No. 238 Jiefang Road, Wuhan 430060, Hubei Province, China. [2]Department of Critical Care Medicine, Renmin Hospital of Wuhan University, No. 238 Jiefang Road, Wuhan 430060, Hubei Province, China. [3]Central Laboratory, Renmin Hospital of Wuhan University, No. 238 Jiefang Road, Wuhan 430060, Hubei Province, China. [4]Department of Gastrointestinal Surgery II, Renmin Hospital of Wuhan University, No. 238 Jiefang Road, Wuhan 430060, Hubei Province, China.

References

1. 2021 Alzheimer's disease facts and figures. Alzheimers Dement. 2021;17(3):327–406.
2. Querfurth HW, Laferla FM. Alzheimer's disease. N Engl J Med. 2010;362(4):329–44.
3. Selkoe DJ. Alzheimer's disease is a synaptic failure. Science. 2002;298(5594):789–91.
4. Wyss-Coray T. Inflammation in Alzheimer disease: driving force, bystander or beneficial response? Nat Med. 2006;12(9):1005–15.
5. Li S, Selkoe DJ. A mechanistic hypothesis for the impairment of synaptic plasticity by soluble Abeta oligomers from Alzheimer's brain. J Neurochem. 2020;154(6):583–97.
6. Benilova I, Karran E, De Strooper B. The toxic Abeta oligomer and Alzheimer's disease: an emperor in need of clothes. Nat Neurosci. 2012;15(3):349–57.
7. Brouillette J, Caillierez R, Zommer N, Alves-Pires C, Benilova I, Blum D, et al. Neurotoxicity and memory deficits induced by soluble low-molecular-weight amyloid-beta1-42 oligomers are revealed in vivo by using a novel animal model. J Neurosci. 2012;32(23):7852–61.
8. Maia LF, Kaeser SA, Reichwald J, Hruscha M, Martus P, Staufenbiel M, et al. Changes in amyloid-beta and Tau in the cerebrospinal fluid of transgenic mice overexpressing amyloid precursor protein. Sci Transl Med. 2013;5(194):194re2.
9. Zhang B, Gaiteri C, Bodea LG, Wang Z, Mcelwee J, Podtelezhnikov AA, et al. Integrated systems approach identifies genetic nodes and networks in late-onset Alzheimer's disease. Cell. 2013;153(3):707–20.
10. Webers A, Heneka MT, Gleeson PA. The role of innate immune responses and neuroinflammation in amyloid accumulation and progression of Alzheimer's disease. Immunol Cell Biol. 2020;98(1):28–41.
11. Chakrabarty P, Li A, Ceballos-Diaz C, Eddy JA, Funk CC, Moore B, et al. IL-10 alters immunoproteostasis in APP mice, increasing plaque burden and worsening cognitive behavior. Neuron. 2015;85(3):519–33.
12. Guillot-Sestier MV, Doty KR, Gate D, Rodriguez JJ, Leung BP, Rezai-Zadeh K, et al. Il10 deficiency rebalances innate immunity to mitigate Alzheimer-like pathology. Neuron. 2015;85(3):534–48.
13. Belarbi K, Jopson T, Tweedie D, Arellano C, Luo W, Greig NH, et al. TNF-alpha protein synthesis inhibitor restores neuronal function and reverses cognitive deficits induced by chronic neuroinflammation. J Neuroinflammation. 2012;9:23.
14. Ghosh S, Wu MD, Shaftel SS, Kyrkanides S, Laferla FM, Olschowka JA, et al. Sustained interleukin-1beta overexpression exacerbates tau pathology despite reduced amyloid burden in an Alzheimer's mouse model. J Neurosci. 2013;33(11):5053–64.
15. Rivera-Escalera F, Pinney JJ, Owlett L, Ahmed H, Thakar J, Olschowka JA, et al. IL-1beta-driven amyloid plaque clearance is associated with an expansion of transcriptionally reprogrammed microglia. J Neuroinflammation. 2019;16(1):261.
16. Vom BJ, Prokop S, Miller KR, Obst J, Kalin RE, Lopategui-Cabezas I, et al. Inhibition of IL-12/IL-23 signaling reduces Alzheimer's disease-like pathology and cognitive decline. Nat Med. 2012;18(12):1812–9.

17. Zhang J, Qiao Q, Liu M, He T, Shi J, Bai X, et al. IL-17 Promotes Scar Formation by Inducing Macrophage Infiltration. Am J Pathol. 2018;188(7):1693–702.
18. Wu HP, Shih CC, Chu CM, Huang CY, Hua CC, Liu YC, et al. Effect of interleukin-17 on in vitro cytokine production in healthy controls and patients with severe sepsis. J Formos Med Assoc. 2015;114(12):1250–7.
19. Burnham SC, Faux NG, Wilson W, Laws SM, Ames D, Bedo J, et al. A blood-based predictor for neocortical Abeta burden in Alzheimer's disease: results from the AIBL study. Mol Psychiatry. 2014;19(4):519–26.
20. Doecke JD, Laws SM, Faux NG, Wilson W, Burnham SC, Lam CP, et al. Blood-based protein biomarkers for diagnosis of Alzheimer disease. Arch Neurol. 2012;69(10):1318–25.
21. Yang J, Kou J, Lalonde R, Fukuchi KI. Intracranial IL-17A overexpression decreases cerebral amyloid angiopathy by upregulation of ABCA1 in an animal model of Alzheimer's disease. Brain Behav Immun. 2017;65:262–73.
22. Reed MD, Yim YS, Wimmer RD, Kim H, Ryu C, Welch GM, et al. IL-17a promotes sociability in mouse models of neurodevelopmental disorders. Nature. 2020;577(7789):249–53.
23. Ushio H, Ishibuchi S, Oshita K, Seki N, Kataoka H, Sugahara K, et al. A new phenylpyrazoleanilide, y-320, inhibits interleukin 17 production and ameliorates collagen-induced arthritis in mice and cynomolgus monkeys. Pharmaceuticals (Basel). 2013;7(1):1–17.
24. Zeng J, Jiang X, Hu XF, Ma RH, Chai GS, Sun DS, et al. Spatial training promotes short-term survival and neuron-like differentiation of newborn cells in Abeta1-42-injected rats. Neurobiol Aging. 2016;45:64–75.
25. Cetin F, Yazihan N, Dincer S, Akbulut G. The effect of intracerebroventricular injection of beta amyloid peptide (1–42) on caspase-3 activity, lipid peroxidation, nitric oxide and NOS expression in young adult and aged rat brain. Turk Neurosurg. 2013;23(2):144–50.
26. Baleriola J, Walker CA, Jean YY, Crary JF, Troy CM, Nagy PL, et al. Axonally synthesized ATF4 transmits a neurodegenerative signal across brain regions. Cell. 2014;158(5):1159–72.
27. Shin E, Kashiwagi Y, Kuriu T, Iwasaki H, Tanaka T, Koizumi H, et al. Doublecortin-like kinase enhances dendritic remodelling and negatively regulates synapse maturation. Nat Commun. 2013;4:1440.
28. D'Acquisto F, Maione F, Pederzoli-Ribeil M, From. IL-15 to IL-33: the never-ending list of new players in inflammation. Is it time to forget the humble aspirin and move ahead? Biochem Pharmacol. 2010;79(4):525–34.
29. Myint L, Wang R, Boukas L, Hansen KD, Goff LA, Avramopoulos D. A screen of 1,049 schizophrenia and 30 Alzheimer's-associated variants for regulatory potential. Am J Med Genet B Neuropsychiatr Genet. 2020;183(1):61–73.
30. Bartsch T, Wulff P. The hippocampus in aging and disease: From plasticity to vulnerability. Neuroscience. 2015;309:1–16.
31. Trost W, Fruhholz S.. Koelsch, et al. The hippocampus is an integral part of the temporal limbic system during emotional processing: Comment on "The quartet theory of human emotions: An

integrative and neurofunctional model" by S. Phys Life Rev. 2015;13:87–8.
32. Fang WL, Zhao DQ, Wang F, Li M, Fan SN, Liao W, et al. Neurotropin(R) alleviates hippocampal neuron damage through a HIF-1alpha/MAPK pathway. Cns Neurosci Ther. 2017;23(5):428–37.
33. Dahlgren KN, Manelli AM, Stine WJ, Baker LK, Krafft GA, Ladu MJ. Oligomeric and fibrillar species of amyloid-beta peptides differentially affect neuronal viability. J Biol Chem. 2002;277(35):32046–53.
34. Jhoo JH, Kim HC, Nabeshima T, Yamada K, Shin EJ, Jhoo WK, et al. Beta-amyloid (1–42)-induced learning and memory deficits in mice: involvement of oxidative burdens in the hippocampus and cerebral cortex. Behav Brain Res. 2004;155(2):185–96.
35. Rueda N, Vidal V, Garcia-Cerro S, Narcis JO, Llorens-Martin M, Corrales A, et al. Anti-IL17 treatment ameliorates Down syndrome phenotypes in mice. Brain Behav Immun. 2018;73:235–51.
36. Meares GP, Ma X, Qin H, Benveniste EN. Regulation of CCL20 expression in astrocytes by IL-6 and IL-17. Glia. 2012;60(5):771–81.
37. Steinman L. A brief history of T(H)17, the first major revision in the T(H)1/T(H)2 hypothesis of T cell-mediated tissue damage. Nat Med. 2007;13(2):139–45.
38. Martinez NE, Sato F, Kawai E, Omura S, Takahashi S, Yoh K, et al. Th17-biased RORgammat transgenic mice become susceptible to a viral model for multiple sclerosis. Brain Behav Immun. 2015;43:86–97.
39. Shankar GM, Li S, Mehta TH, Garcia-Munoz A, Shepardson NE, Smith I, et al. Amyloid-beta protein dimers isolated directly from Alzheimer's brains impair synaptic plasticity and memory. Nat Med. 2008;14(8):837–42.
40. Forloni G, Artuso V, La Vitola P, Balducci C. Oligomeropathies and pathogenesis of Alzheimer and Parkinson's diseases. Mov Disord. 2016;31(6):771–81.
41. Cristiano C, Volpicelli F, Lippiello P, Buono B, Raucci F, Piccolo M, et al. Neutralization of IL-17 rescues amyloid-beta-induced neuroinflammation and memory impairment. Br J Pharmacol. 2019;176(18):3544–57.
42. Miossec P, Kolls JK. Targeting IL-17 and TH17 cells in chronic inflammation. Nat Rev Drug Discov. 2012;11(10):763–76.
43. Gelderblom M, Weymar A, Bernreuther C, Velden J, Arunachalam P, Steinbach K, et al. Neutralization of the IL-17 axis diminishes neutrophil invasion and protects from ischemic stroke. Blood. 2012;120(18):3793–802.
44. Swardfager W, Winer DA, Herrmann N, Winer S, Lanctot KL. Interleukin-17 in post-stroke neurodegeneration. Neurosci Biobehav Rev. 2013;37(3):436–47.
45. Vassar R, Kuhn PH, Haass C, Kennedy ME, Rajendran L, Wong PC, et al. Function, therapeutic potential and cell biology of BACE proteases: current status and future prospects. J Neurochem. 2014;130(1):4–28.
46. Shin RW, Ogino K, Shimabuku A, Taki T, Nakashima H, Ishihara T, et al. Amyloid precursor protein cytoplasmic domain with phospho-Thr668 accumulates in Alzheimer's disease and its transgenic

models: a role to mediate interaction of Abeta and tau. Acta Neuropathol. 2007;113(6):627–36.

47. Triaca V, Sposato V, Bolasco G, Ciotti MT, Pelicci P, Bruni AC, et al. NGF controls APP cleavage by downregulating APP phosphorylation at Thr668: relevance for Alzheimer's disease. Aging Cell. 2016;15(4):661–72.
48. Chang KA, Kim HS, Ha TY, Ha JW, Shin KY, Jeong YH, et al. Phosphorylation of amyloid precursor protein (APP) at Thr668 regulates the nuclear translocation of the APP intracellular domain and induces neurodegeneration. Mol Cell Biol. 2006;26(11):4327–38.

Figures

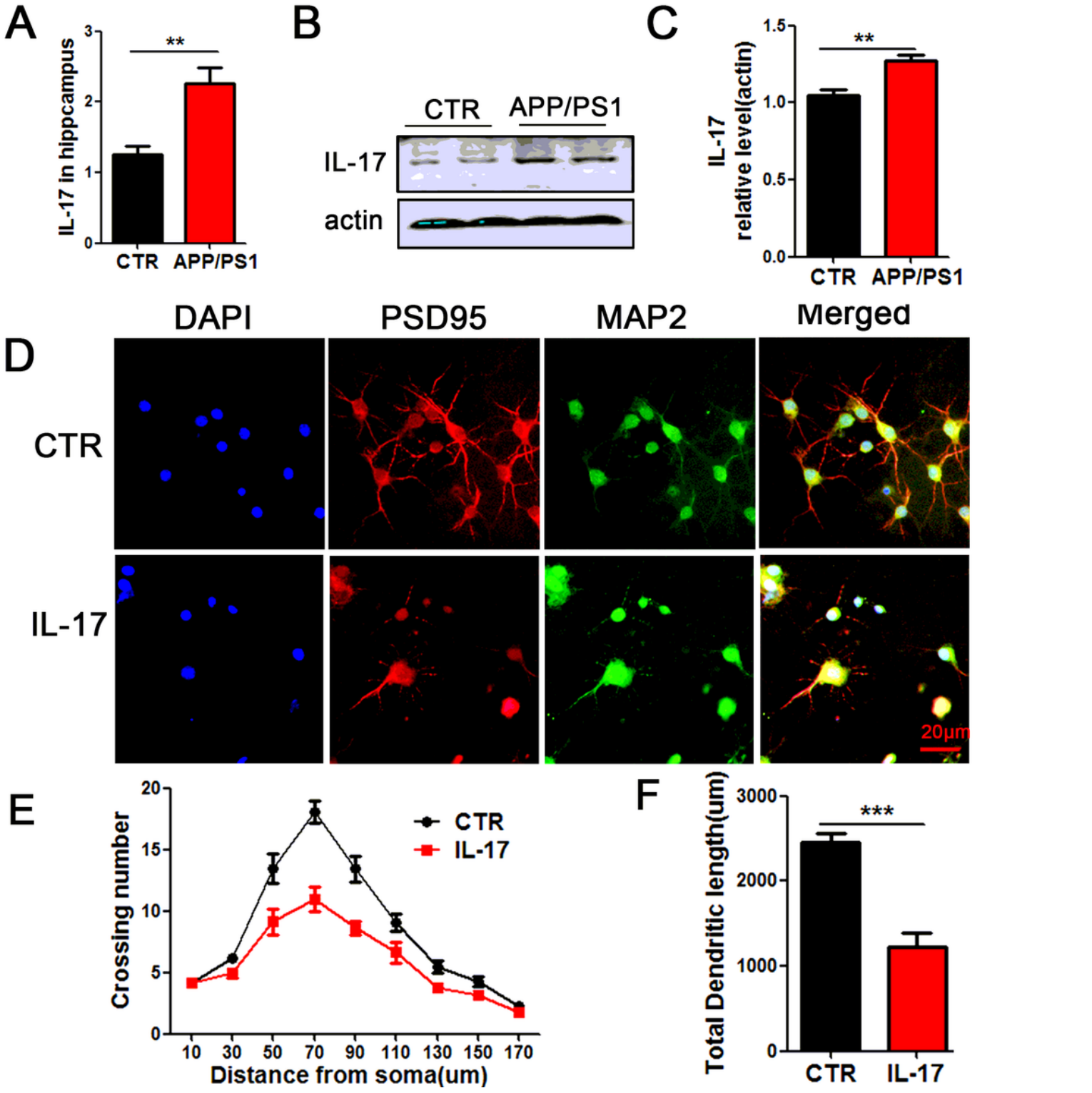

Figure 1

IL-17 is up-regulated in APP/PS1 transgenic mice and induces neural toxicity. (A) Result from ELISA tests, the level of IL-17 in APP/PS1 mice (n = 6) and WT control mice hippocampus (n = 6). Representative western blotting (B) and quantification of IL-17 (C) expression were shown. (D–F) Mice's primary hippocampal neurons were treated with DMSO for control and IL-17 for model for 7 d. The neuronal morphology changes were measured by immunofluorescent staining of anti-PSD95 and anti-MAP2

antibodies. Representative images after treatment (D, Scale bar = 20 μm), Sholl analysis (E), quantitative analyses of dendritic length (F), n = 16 hippocampal neurons. All data are presented as mean ± SEM. *p < 0.05, **p < 0.01, and ***p < 0.001 versus control

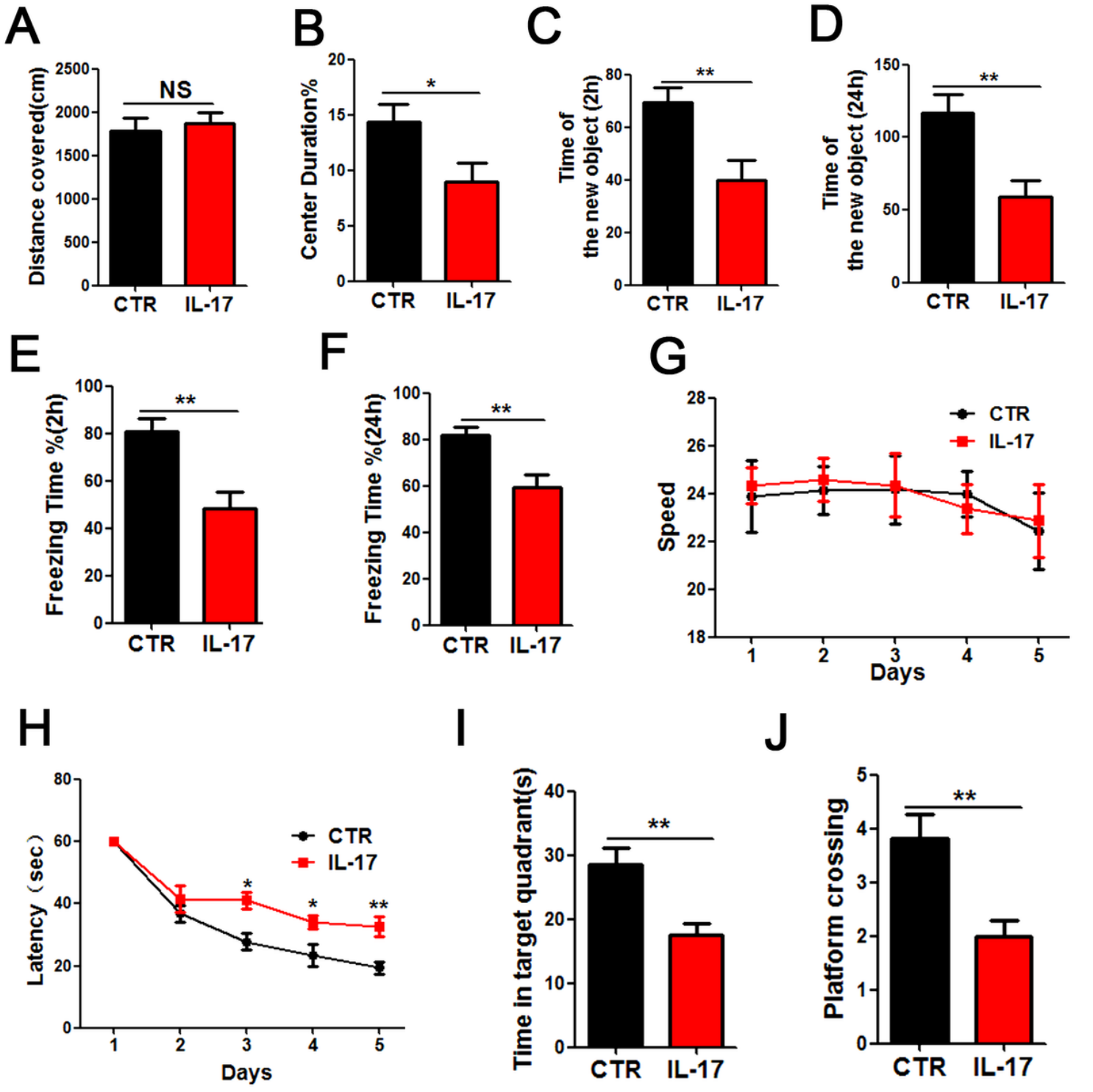

Figure 2

IL-17 results in cognitive and memory impairments in mice. Thirty healthy wild type C57BL mice were stereotaxically injected in the lateral ventricle with IL-17 (IL-17 group, 100 μg/mL, 5 μL) or saline (control group, 5 μL) for 1 week. Series behavioral tests were performed. (A, B) The open field showed no

difference in the total distance covered (A), but a significant decrease in the time of center duration (B) in IL-17 treated group. (C, D) Novel object recognition test (NORT) showed the measured recognition time of new object in 2 h (C) and 24 h (D). (E, F) Contextual fear conditioning test found out the freezing time in 2 h (E) and 24 h (F). (G-J) The Morris water maze test (MWM): the speed in the water (G) and the latency to find the hidden platform from day 1 to day 5 (H), the time spent in the target quadrant (I) and the number of the position of target platform crossing (J) were measured. All data are presented as mean ± SEM. *p < 0.05, **p < 0.01, and ***p < 0.001 versus control

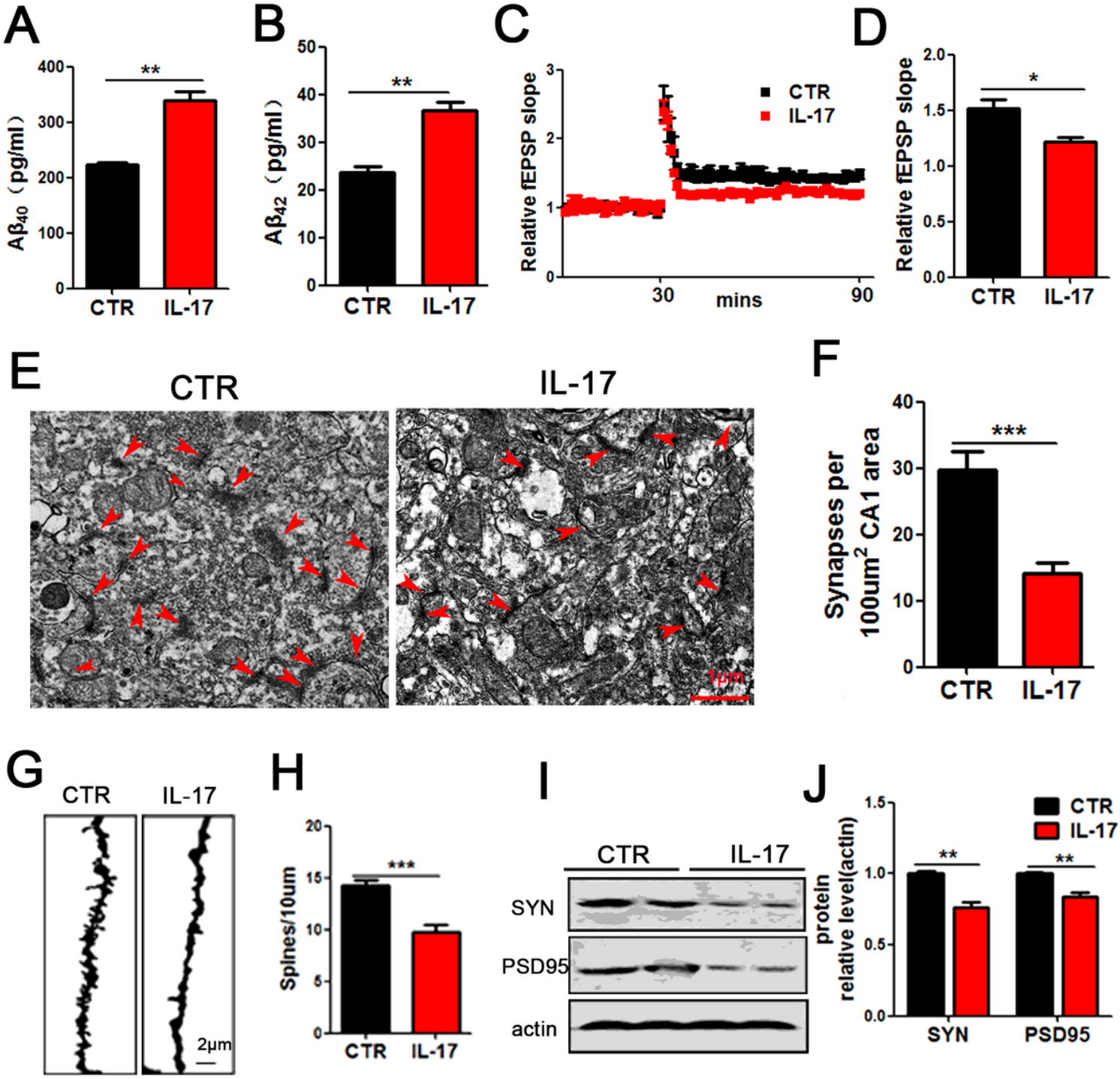

Figure 3

IL-17 induces synaptic dysfunction in hippocampus accompanying with Aβ overproduction. WT C57BL mice were given IL-17 or saline control. Levels of Aβ40 (A) and Aβ42 (B) in hippocampus were test by ELISA in IL-17 group mice and control group mice. (C, D) Normalized CA3-CA1 fEPSP mean slope recorded from CA1 dendritic region in acute hippocampal slices (C). Quantitative analyses of normalized fEPSP slope (D). n = 10, 5 mice per group, 5 brain slices per mouse were recorded. (E, F) Transmission electron microscopy (TEM) showed the structure of synapses. Red arrows indicated the structure of the presynaptic and postsynaptic membranes, and the synaptic cleft synapses (E). Scale bar = 500 nm. Quantitative analyses of the number of synapses (F). (G, H) Representative images of dendritic spines of neurons from Golgi impregnated hippocampus (G); averaged spine density (mean spine number per 10-mm dendrite segment) was measured in mice (H). Scale bar = 2 μm. (I, J) SYN and PSD95 expression levels were detected by western blotting using specific antibodies, and actin was used as a loading control (I). Intensity analysis of SYN and PSD95 levels (J). All data represent mean ± SEM. *$p < 0.05$, **$p < 0.01$, and ***$p < 0.001$ versus control

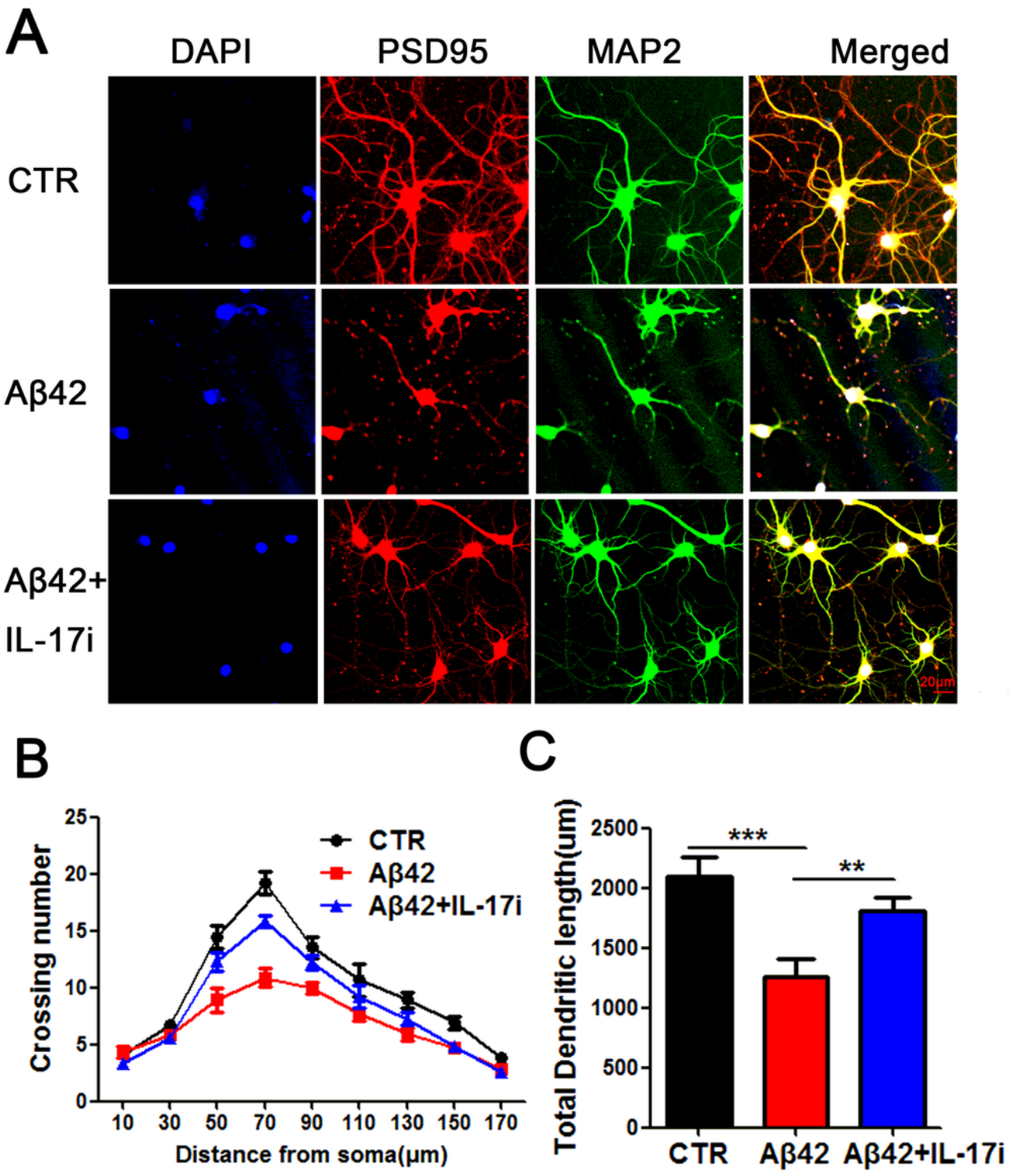

Figure 4

IL-17 inhibitor (Y-320) ameliorates Aβ42-induced neural toxicity in primary hippocampal neurons. Mice primary hippocampal neurons at DIV 9 were treated with DMSO, Aβ42, and Aβ42 + IL-17 inhibitor, and the neuronal morphology were measured by immunofluorescent staining of anti-PSD95 and anti-MAP2 antibodies. Representative images after treatment (A), Sholl analysis (B), quantitative analysis of

dendritic length (C), scale bar = 20 μm. n = 16 hippocampal neurons. All data represent as mean± SEM. *p < 0.05, **p < 0.01, and ***p < 0.001 versus model group

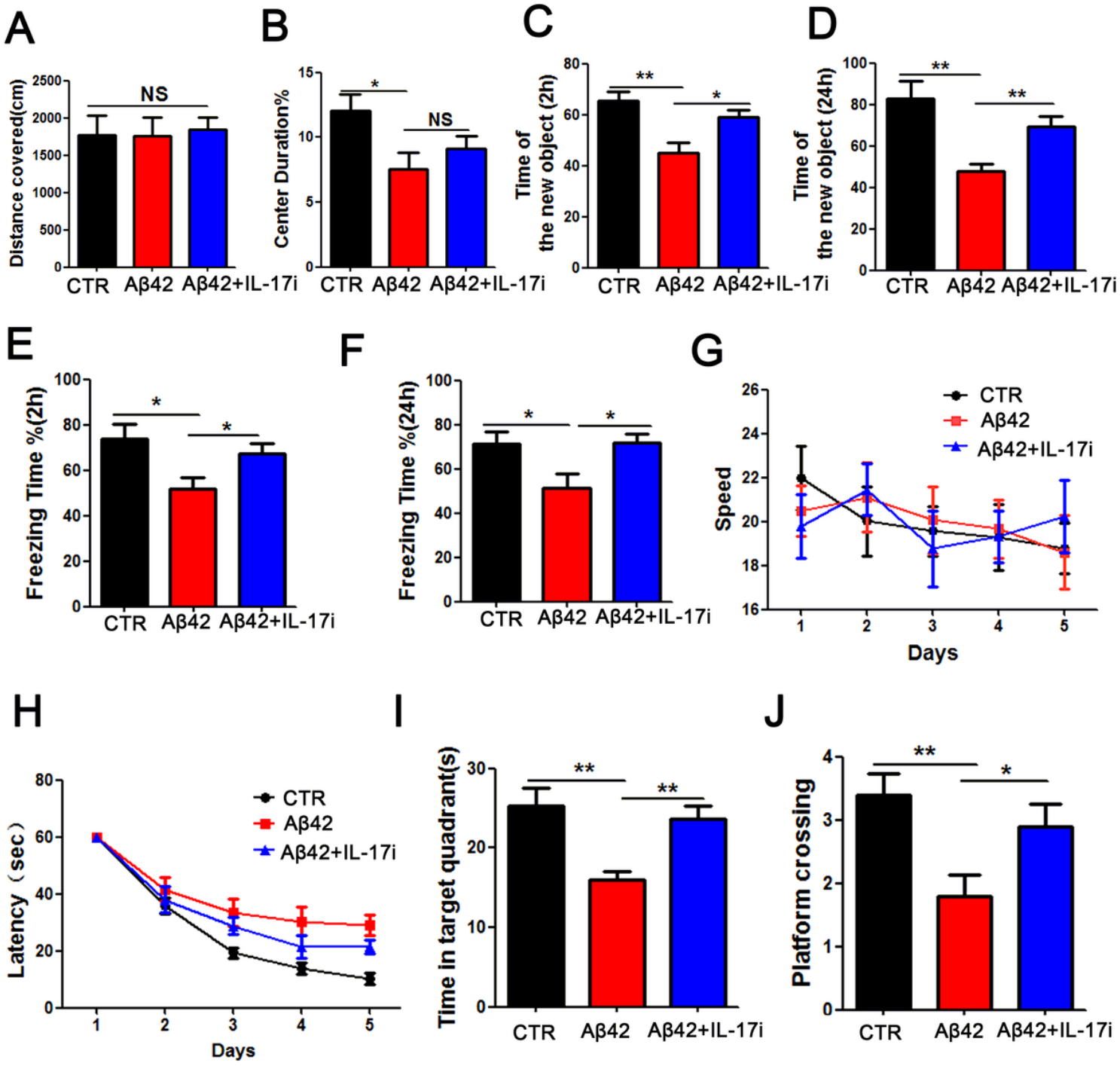

Figure 5

IL-17 inhibitor alleviates Aβ42-induced cognitive and memory deficits in mice. Forty-five healthy C57BL mice were randomly divided into 3 groups. In the control group, 15 mice were injected with saline in brain lateral ventricle. Another 15 mice were injected with Aβ42 (2.0 μg/μL, 5 μL) in brain lateral ventricle to serve as Aβ42 model group, while the last 15 mice were injected with Aβ42 and then treatment with Y-320 (3 mg/kg, 7 days) by oral gavage to serve as Aβ42 + IL-17 inhibitor group. (A, B) The open field test

showed he total distance covered (A), and the time of center duration (B) the three groups. (C, D) NORT showed the time spent exploring new objects 2 h (C) and 24 h (D). (E, F) Contextual fear conditioning test found out the freezing time in 2 h (E) and 24 h (F). (G-J) MWM test: the speed in the water (G) and the latency to find the hidden platform from day 1 to day 5 (H) on training, the time spent in the target quadrant (I) and the number of the position of target platform crossing (J) were shown. All data are presented as mean ± SEM. *p < 0.05, **p < 0.01, and ***p < 0.001 versus model group

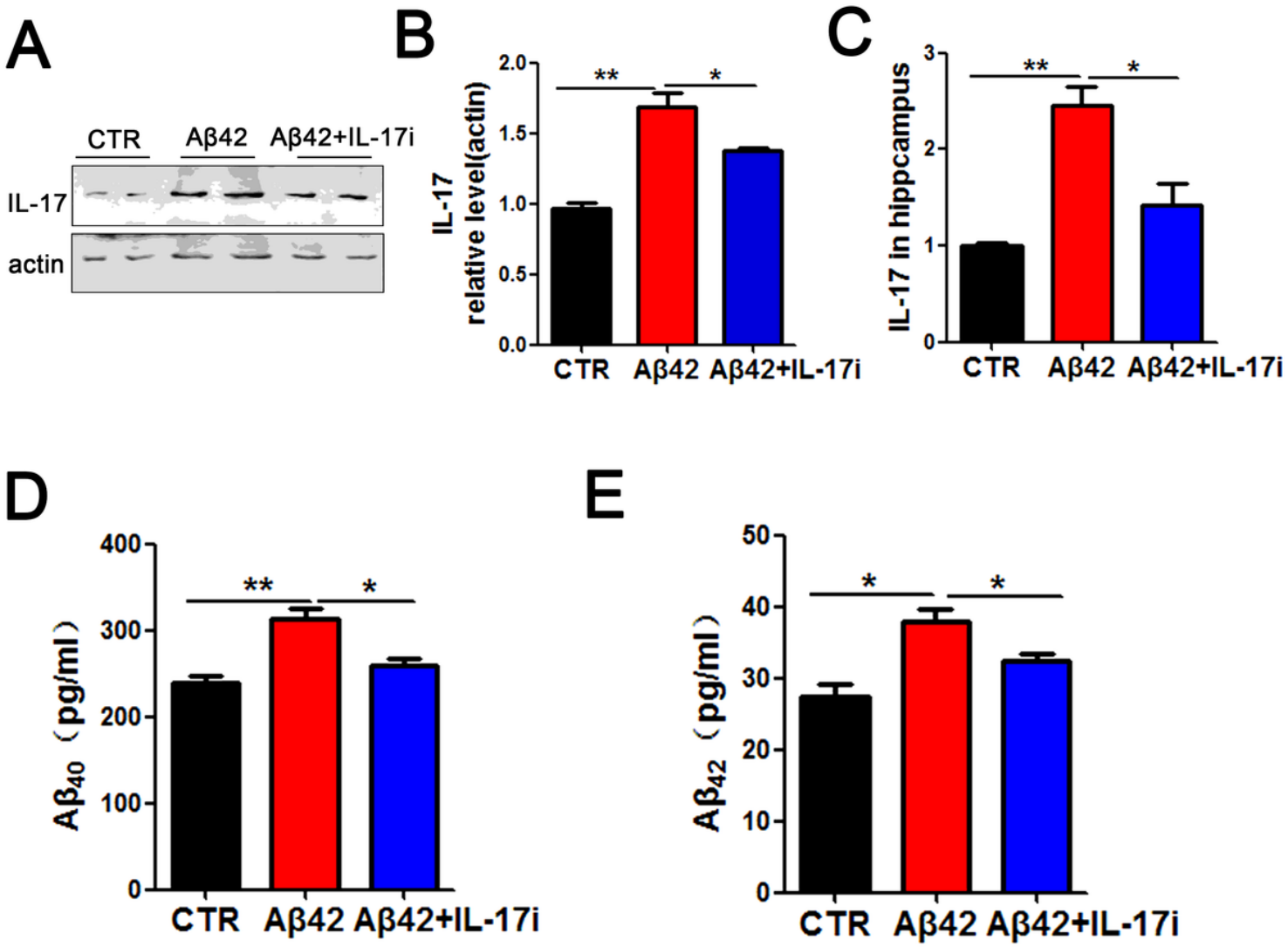

Figure 6

IL-17 inhibitor decreases Aβ generation in Aβ42-induced AD-like pathology. (A, B) Brain tissues (hippocampus) were homogenized and IL-17 protein level was detected by immnuoblotting. Actin was used as a loading control (A). Quantitative analyses of the IL-17 level (B). ELISA assays to measure levels of IL-17 (C), Aβ40 (D) and Aβ42 (F) of hippocampus in groups. n = 6 for all groups; all data are presented as mean ± SEM. *p < 0.05, **p < 0.01, and ***p < 0.001 versus Aβ42 model group

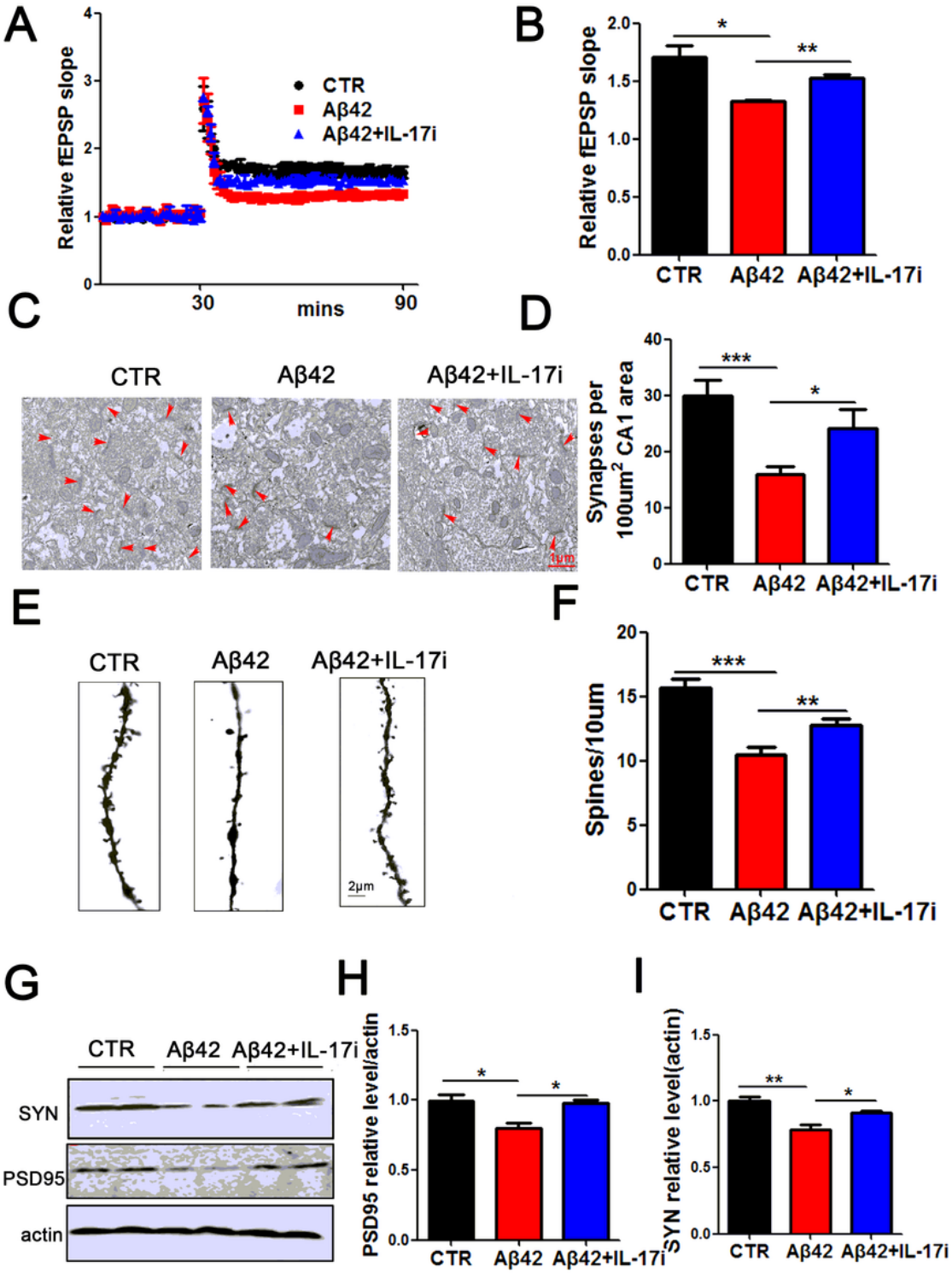

Figure 7

IL-17 inhibitor rescues Aβ42-induced spine Loss and synaptic dysfunction. (A, B) Normalized CA3-CA1 fEPSP mean slope recorded from CA1 dendritic region in acute hippocampal slices (A). Quantitative analysis of normalized fEPSP slops (B). n = 12, 4 mice per group, 5 brain slices per mouse were recorded. (C, D) TEM showed the structure of synapses. Red arrows indicated the structure of the presynaptic and postsynaptic membranes, and the synaptic cleft (C). Scale bar = 500 nm. Quantitative analyses of the

number of synapses (D). (E, F) Representative images of dendritic spines of neurons from Golgi staining hippocampus (E); averaged spine density (mean spine number per 10-mm dendrite segment) was measured in mice (F). Scale bar = 2 μm. (G-I) PSD95 and SYN expression levels were detected by western blotting using specific antibodies, and actin was used as a loading control (G). Intensity analysis of PSD95 (H) and SYN levels (I). All data represent mean ± SEM. *p < 0.05, **p < 0.01, and ***p < 0.001 versus Aβ42 model group

Supplementary Files

This is a list of supplementary files associated with this preprint. Click to download.

- sFig.1.tif
- sFig.2.tif
- sFig.3.tif